Transferability of Quantum Topological Atoms in Terms of Electrostatic Interaction Energy

Michel Rafat, Majeed Shaik, and Paul L. A. Popelier*

School of Chemistry, University of Manchester Faraday Building, North Campus Manchester M60 1QD, Great Britain

Received: August 12, 2006; In Final Form: October 6, 2006

Understanding atomic transferability is important to guide the design of a force field. Atoms in molecules are defined and computed according to the theory of quantum chemical topology (QCT). The electron density associated with such topological atoms is conveniently described by high-rank multipole moments. Here, we assess the transferability of atoms by means of their electrostatic interaction energy, using a convergent multipole expansion. The test systems are $(H_2O)_3$ and serine...$(H_2O)_5$. The effect of a varying electron density cutoff (i.e., truncating the atoms) is discussed and the effect of polarization is quantified.

Introduction

The existence of functional groups in chemistry is due to the approximate transferability of atomic properties. Indeed, atoms in nearly identical chemical environments share nearly identical properties. Quantifying transferability requires a robust definition of an atom. Of the various alternatives summed up in a recent paper on functional group transferability,[1] this work adopts the definition by the theory of quantum chemical topology (QCT).[2,3] This theory delineates an atom within its molecular environment by means of the gradient vector field of the electron density. A series of recent studies[4−9] have systematically addressed the transferability of quantum topological atomic and bond properties in certain classes of organic molecules.

The transferability of atomic properties is especially important in large molecules or clusters (including liquids) where a complete ab-initio treatment is not achievable. This is where force fields (still) have an important role to play. Proteins in particular received considerable attention. Matta and Bader studied the use of amino acids as building blocks,[10−12] whereas Popelier and Aicken computed quantum topological atom types[13−15] for amino acids. Using the topological partitioning of the electron density, Breneman and co-workers designed a method, coined transferable atom equivalent[16,17](TAE), which can rapidly reconstruct a molecule by adjusting the interatomic surface between two atoms of a TAE library.

Over the past few years, we have systematically addressed key questions arising in our endeavor of constructing a fully multipolar and polarizable QCT force field for proteins in water. This article considers a particular aspect arising in this construction. Some years ago, we started by demonstrating that QCT multipole moments lead to a convergent series expansion of the electrostatic potential[18] and the reason why.[19] Two separate and new ideas, that is, continuous (Bessel) moments[20] and inverse moments,[21] enabled enlargement of the convergence sphere. Within the context of long-range perturbation theory, the electrostatic interaction between topological atoms could also be successfully expressed as a convergent multipole expansion and could therefore be used in the prediction of van der Waals complexes[22] and hydrogen-bonded DNA base pairs.[23] In a (super)molecular context, the convergence of the atomic multipole expansion of intramolecular and intermolecular Coulomb energy also proved satisfactory.[24] A companion study[25] confirmed the convergence of both exchange energies and forces, now examined at higher multipole ranks. Returning to the Coulomb interaction, it emerged that both 1,3 and 1,4 interactions can be described on the same footing as 1,n (n > 4) interactions by a convergent multipole expansion.[26] Subsequently, a paper[27] on QCT partitioning of the total energy highlighted the importance of self-energy terms (kinetic and intra-atomic Coulomb and exchange). Concerns about the efficiency and practicality of a high-rank multipolar force field was addressed in work[28] that determined which rank is necessary to have the electrostatic energy converge to the exact interaction energy within a certain error margin.

Here, we focus on atomic transferability in terms of their electrostatic (Coulomb) interaction energy. There are different levels of assessing this transferability. The most direct level is to compare the multipole moments themselves for they are the ultimate descriptors of the electron density associated with a topological atom. This route was followed by Popelier and Aicken in their computation of atom types.[15] The next level of transferability assessment uses the electrostatic potential generated by a topological atom. Here, the advantage is that its transferability can be quantified by a single number (expressed as energy per unit charge), rather than by a set of numbers, one for each multipole moment. The disadvantage is that a grid of points needs to be specified to assess the transferability. This level of transferability assessment was followed before[1] and showed how functional groups are better isolated by an aliphatic chain rather than by a conjugated one. In this study, the transferability of electrostatic moments is assessed through the electrostatic energy. Here, the advantage is that no grid specification is required. However, one needs a set of atoms that a given atom (whose transferability is investigated) interacts with.

In this contribution, we answer two concrete questions. The first question relates to the outer boundary of a topological atom, which determines the volume over which property densities are integrated, resulting in atomic multipole moments. How does the atom−atom interaction energy change if the atomic volume is reduced by capping it by an envelope of higher electron density than the reference value of $\rho = 10^{-7}$ au? The second

* Author to whom correspondence should be addressed. E-mail: pla@manchester.ac.uk.

10.1021/jp0652190 CCC: $33.50
Published on Web 11/23/2006

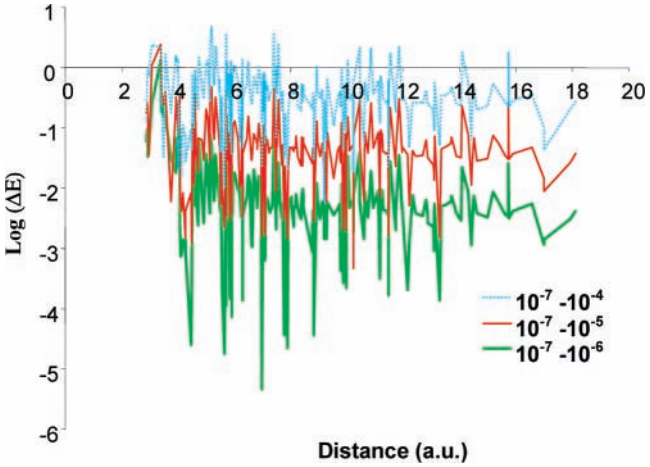

Figure 1. Difference in the atomic electrostatic energies in the serine...water cluster calculated with isodensity cutoff at 10^{-7} au and 10^{-4}, 10^{-5}, and 10^{-6} au as a function of the internuclear distance. The energy is expressed as $10^{\log(\Delta E)}$ kJ/mol.

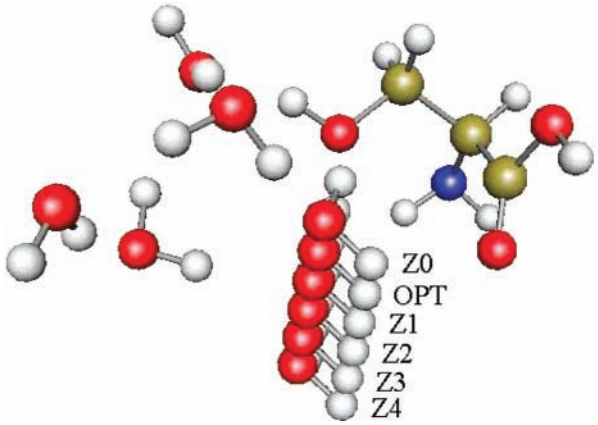

Figure 2. New positions *z*0, *z*1, *z*2, *z*3, and *z*4 of the water molecule in the serine...$(H_2O)_5$ cluster. The position OPT refers to the optimized configuration.

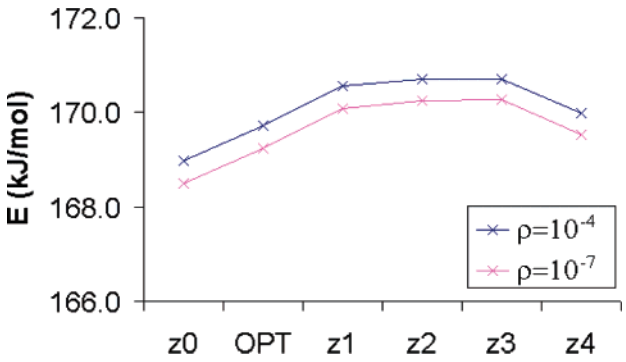

Figure 3. Total electrostatic energy between the atoms from the serine...water cluster integrated with atomic volumes capped at $\rho = 10^{-7}$ au and at $\rho = 10^{-4}$ au.

question concerns the difference in atom−atom interaction energy calculated from the atomic multipole moments of a supermolecule and the moments obtained from its separated molecular fragments, each one with its own wave function.

We investigate two systems of interest: the water trimer, $(H_2O)_3$, and a hydrated serine complex, Ser...$(H_2O)_5$. While the exact choice of systems is arbitrary, it is guided by the importance of water in life and, in particular, by the hydration of proteins. Because of computational demands associated with our analysis, we were restricted to the current systems, which we hope are representative enough to shed light on the problem of transferability in terms of interaction energy.

Computational Details

By integrating over an atomic volume the electron density multiplied by the corresponding regular spherical harmonics,[29] one obtains the atomic multipole moments. The Coulomb interaction between two atoms is then given[22] by eq 1,

$$E(\mathrm{A},\mathrm{B}) = \sum_{l_A=0}^{\infty}\sum_{l_B=0}^{\infty}\sum_{m_A=-l_A}^{l_A}\sum_{m_B=-l_B}^{l_B} T_{l_A m_A l_B m_B}(\mathbf{R})\, Q_{l_A m_A}(\Omega_A)\, Q_{l_B m_B}(\Omega_B) \quad (1)$$

where $Q_{l_A m_A}(\Omega_A)$ and $Q_{l_B m_B}(\Omega_B)$ designated the moments of atom A and B, respectively, and the index l refers to the rank of the multipole moments. Each atom has its own local axis system, centered on the nucleus. The symbol T(**R**) denotes the interaction tensor and **R** the vector linking the nuclear positions of the respective atoms (i.e., the origins of their local frames). The terms of eq 1 can be collected according to powers of $R = |\mathbf{R}|$ by means of a rank called L, which is defined as $l_A + l_B + 1$. The convergence of the multipole expansion can be monitored against a varying rank L.

Using GAUSSIAN03,[30] the water and serine complex were optimized at B3LYP/6-311G+(2d,p) level, which offers a good compromise between speed and accuracy.[24] All the atoms were integrated with MORPHY01.[31] For the water trimer, the quadrature inside the β-sphere was set to $(n_r, n_\theta, n_\varphi) = (90, 60, 90)$, giving the number of radial and angular quadrature points, respectively. For the rest of the atom, we used the same grid. For the serine complex, the β-sphere quadrature was $(n_r, n_\theta, n_\varphi) = (90, 30, 50)$ and outside the β-sphere $(n_r, n_\theta, n_\varphi) = (120, 90, 140)$. The atomic volumes were capped at the constant electron density envelope of $\rho = 10^{-7}$, 10^{-6}, 10^{-5}, and 10^{-4} au. The moments were computed up to rank $l = 20$. All atoms in the water trimer were successfully integrated at all isodensity values, but in the serine complex four atoms (C2, O14, O15, and O21, Figure 6) failed at $\rho = 10^{-7}$ au and three more atoms (H9, O12, and H23, Figure 6) at $\rho = 10^{-4}$ au. As one of the water molecules was moved in the serine...water cluster (see Figure 2), four more atoms (C3, O10, O24, and O27, Figure 6) failed to integrate because of intricate topologies. Evidently, we only considered convergent atom−atom interactions. It was established[32] that the energies obtained at expansion rank $L = l_A + l_B + 1 = 10$ deviate least from the "exact" energy, obtained by six-dimensional integration over two atomic volumes. We define a multipole expansion to be convergent at rank L if the difference between the expansions at the ranks L, L-1, L-2 and the "exact" reference energy is less than 0.1 kJ/mol, which is a rather severe criterion. This value represents the accuracy of the converged multipole expansion. None of the 1,2 interactions converged, and the 1,3 interactions could have satisfied a less severe convergence criterion. As a consequence, in the water trimer, only 21 out of $36 = (9 \times 8)/2$ possible interactions were considered and only 194 interactions in the serine...water complex were considered. At $\rho = 10^{-7}$ au, virtually all electron density is included in the atomic integration, and therefore the multipole moments reach their limiting value. This also means that the corresponding interaction energy reaches its limiting value and will hence be used as the reference for all comparisons described in the next section.

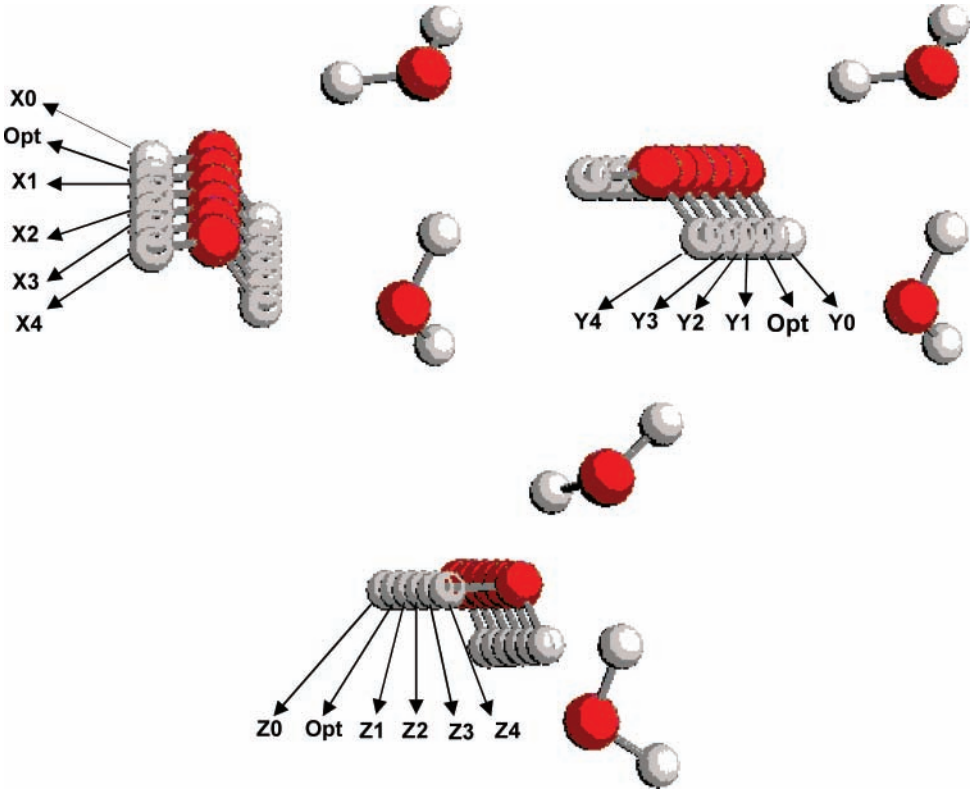

Figure 4. New positions of one water molecule in the trimer, along the *x*, *y*, and *z*-axes. The position Opt refers to the optimized configuration.

Results and Discussion

We start by comparing atom−atom electrostatic interaction energies calculated after capping the atom at $\rho = 10^{-6}$, 10^{-5}, and 10^{-4} au with energies calculated at the reference capping of $\rho = 10^{-7}$ au. In the Ser...$(H_2O)_5$ system, there are a sufficient number of atoms, separated by various internuclear distances, to obtain trends in such a comparison. In Figure 1, we plotted the absolute difference between the atomic interaction energies for each of the three cappings ($\rho = 10^{-6}$, 10^{-5}, and 10^{-4} au). Disregarding the fluctuations, the three ΔE profiles are spaced by about 1 log unit. So, as the cutoff electron density increases by a factor of 10, the energy difference also increases by a factor of 10.

The maximum difference between the energies at $\rho = 10^{-7}$ au and $\rho = 10^{-6}$ au is 0.07 kJ/mol, while the maximum difference between the isodensities $\rho = 10^{-7}$ au and $\rho = 10^{-5}$ au is still less than 0.5 kJ/mol. However, between $\rho = 10^{-7}$ and $\rho = 10^{-4}$ au, the difference can reach up to 4 kJ/mol and often more than 1 kJ/mol. One might conclude that the moments of the atoms defined by a boundary at $\rho = 10^{-4}$ au cannot accurately represent the energy of the atoms defined at $\rho = 10^{-7}$ au.

In the light of this finding, it is important to establish whether the moments defined at $\rho = 10^{-4}$ au can nevertheless represent the variation of the energy upon a change in molecular geometry. In other words, how is the potential energy landscape modified by a difference in the electron density capping the atom? To answer this question, we changed the position of one water molecule in the Ser...$(H_2O)_5$ cluster (along an axis arbitrarily called *z*) leading to five new configurations denoted by *z*0, *z*1, *z*2, *z*3, and *z*4 (see Figure 2). The oxygen atom O15 (in Figure 6) is translated in steps of 1 au, corresponding to shifts of the lower middle water molecule in Figure 2.

For each configuration, we successfully integrated 18 atoms up to the boundary of $\rho = 10^{-7}$ au and again up to the $\rho = 10^{-4}$ au boundary. Although more than 18 integrated atoms were available at $\rho = 10^{-7}$ au, the extra atoms were discarded to keep the number of atoms consistent between the cutoff values. For each configuration, we added the interaction energy between each of the 18 atoms and all other possible atoms of the list of 18, provided that interaction energy converged. Each interaction is counted only once. The summed interaction energy profiles are shown in Figure 3.

At $\rho = 10^{-4}$ au, the moments overestimate the energy by about 0.5 kJ/mol. However, the important observation is that this difference remains constant for all configurations. The potential energy profile obtained at $\rho = 10^{-4}$ au is simply shifted to that obtained at $\rho = 10^{-7}$ au. Hence, we expect that the multipole moments at $\rho = 10^{-4}$ au can also be used to locate extrema on the potential energy surface. To generalize this conclusion, we reinvestigate the same question by means of the water trimer. Here, all atoms integrated successfully. In this system, one water molecule is shifted in three mutually perpendicular directions (arbitrarily called *x*, *y*, and *z*), as shown in Figure 4. The oxygen atom O2 is translated in steps of 0.1 Å, corresponding to the stepwise shift of the left water molecule.

For each configuration, we again added the interaction energy between each of the nine atoms and all other possible atoms of the list of nine, provided that interaction energy converged. Each interaction is counted only once. The summed interaction energy profiles are shown in Figure 5. Figure 5a shows the energy profile for the shift of one water molecule along one axis (the "*y*-axis" in Figure 4). On this scale, the profiles corresponding to $\rho = 10^{-7}$, 10^{-6}, and 10^{-5} au virtually coincide (although the difference between $\rho = 10^{-5}$ and 10^{-7} can amount up to 1.6 kJ/mol). The $\rho = 10^{-4}$ au and $\rho = 10^{-3}$ au curves increasingly underestimate the interaction energy. Figure 5b shows the difference between the profiles and their reference profile at $\rho = 10^{-7}$ au. Again, as with the serine...water complex, the differences are nearly constant. On average, the four energy

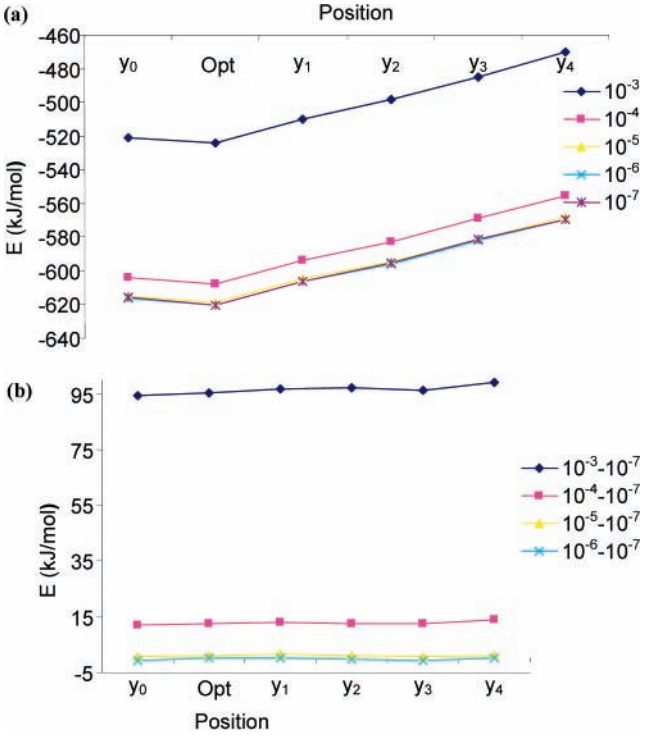

Figure 5. (a) Total electrostatic energy for the water trimer with atoms integrated up to the boundaries $\rho = 10^{-3}$, 10^{-3}, 10^{-4}, 10^{-5}, and 10^{-6} and $\rho = 10^{-7}$ au as a function of position of one water molecule shifted along the *y*-axis (see Figure 4). (b) Difference in total electrostatic energy for the water trimer between the isodensity envelope $\rho = 10^{-7}$ au and 10^{-3}, 10^{-4}, 10^{-5}, and 10^{-6} au as a function of position of one water molecule shifted along the *y*-axis.

TABLE 1: Transferability of Electrostatic Interaction Energy between Atoms in Ser...$(H_2O)_5$ for Two Different Electron Density Cutoff Values[a]

	ρ_{cutoff}	
atom	10^{-4} au	10^{-7} au
C1	2.1	2.3
C3	9.2	6.7
N4	3.6	3.5
H5	1.6	1.6
H6	2.2	1.5
H7	1.9	1.8
H8	2.8	3.2
H9	n/a	2.7
O10	20.3	17.3
H11	19.3	19.4
O12	n/a	5.2
H13	2.7	2.7
H16	12.2	12.5
H17	3.2	3.4
O18	3.3	3.4
H19	5.9	5.6
H20	7.4	7.2
H22	4.2	3.1
H23	n/a	6.3
O24	8.3	6.3
H25	3.7	3.7
H26	5.1	6.6
O27	5.6	5.3
H28	3.1	2.9
H29	2.4	2.1
overall average	5.9	5.4

[a] Average of absolute energy differences between an atom in the supermolecule (interacting with other atoms) and the same atom in either of the two separate fragments (serine and $(H_2O)_5$).

profiles log(ΔE) in Figure 1 are spaced by about 1 log unit. So, as for the serine...water complex, the energy difference

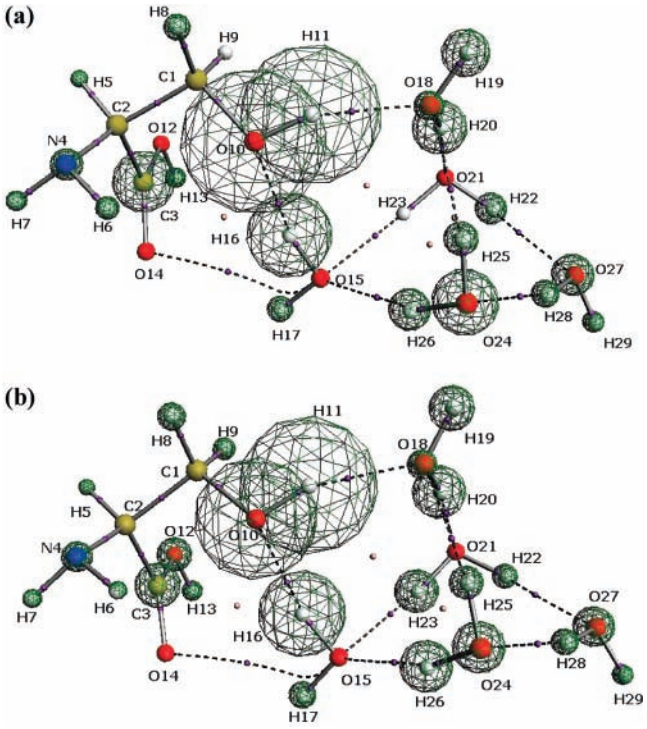

Figure 6. Transferability of atomic multipole moments in the serine...-$(H_2O)_5$ cluster with a cutoff of (a) $\rho = 10^{-4}$ au and (b) $\rho = 10^{-7}$ au. The size of the triangulated spheres represents the average energy difference between the interactions of supermolecule and the fragments. Atoms without a sphere failed to integrate but the sphere around C1 is exactly the same size as the ball representing its nucleus.

TABLE 2: Transferability of Electrostatic Interaction Energy between Atoms in $(H_2O)_3$ for Five Different Electron Density Cutoff Values[a]

	ρ_{cutoff}				
atom	10^{-3} au	10^{-4} au	10^{-5} au	10^{-6} au	10^{-7} au
H1	5.5	5.2	5.2	5.2	5.2
O2	20.8	16.4	14.1	15.1	15.1
H3	18.5	22.1	22.8	22.9	23.0
O4	9.0	7.0	6.5	6.5	6.5
H5	9.4	9.6	9.1	9.7	9.7
H6	13.7	14.0	14.0	14.0	14.1
O7	18.9	19.8	19.9	19.9	19.9
H8	5.9	4.9	4.6	4.6	4.6
H9	12.6	15.2	15.6	15.7	15.8
overall average	12.7	12.7	12.4	12.6	12.6

[a] Average of absolute energy differences between an atom in the supermolecule (interacting with other atoms) and the same atom in one of the two separate fragments (H_2O and $(H_2O)_2$).

increases by approximately 1 order of magnitude as the cutoff electron density increases by an order of magnitude. The conclusions drawn from the energy profiles from the two other mutually perpendicular shifts (the "*x*-axis" and the "*z*-axis" in Figure 4) are the same. Overall, we confirm and thus generalize the conclusion drawn from the Ser...water complex that energy profiles corresponding to the $\rho = 10^{-4}$ au cutoff and even the $\rho = 10^{-3}$ au cutoff mimic the profile at the reference $\rho = 10^{-7}$ au cutoff. Overall, this means that "truncating" an atom according to cutoff values orders of magnitude higher than $\rho = 10^{-7}$ au can be justified if one is interested in relative energy differences, which constitute the majority of applications anyway. Furthermore, the higher the value of the cutoff electron density value, the more transferable an atom's shape becomes. This is because more truncated atoms (i.e., higher ρ) are imprinted with less features of the molecule they are part of.

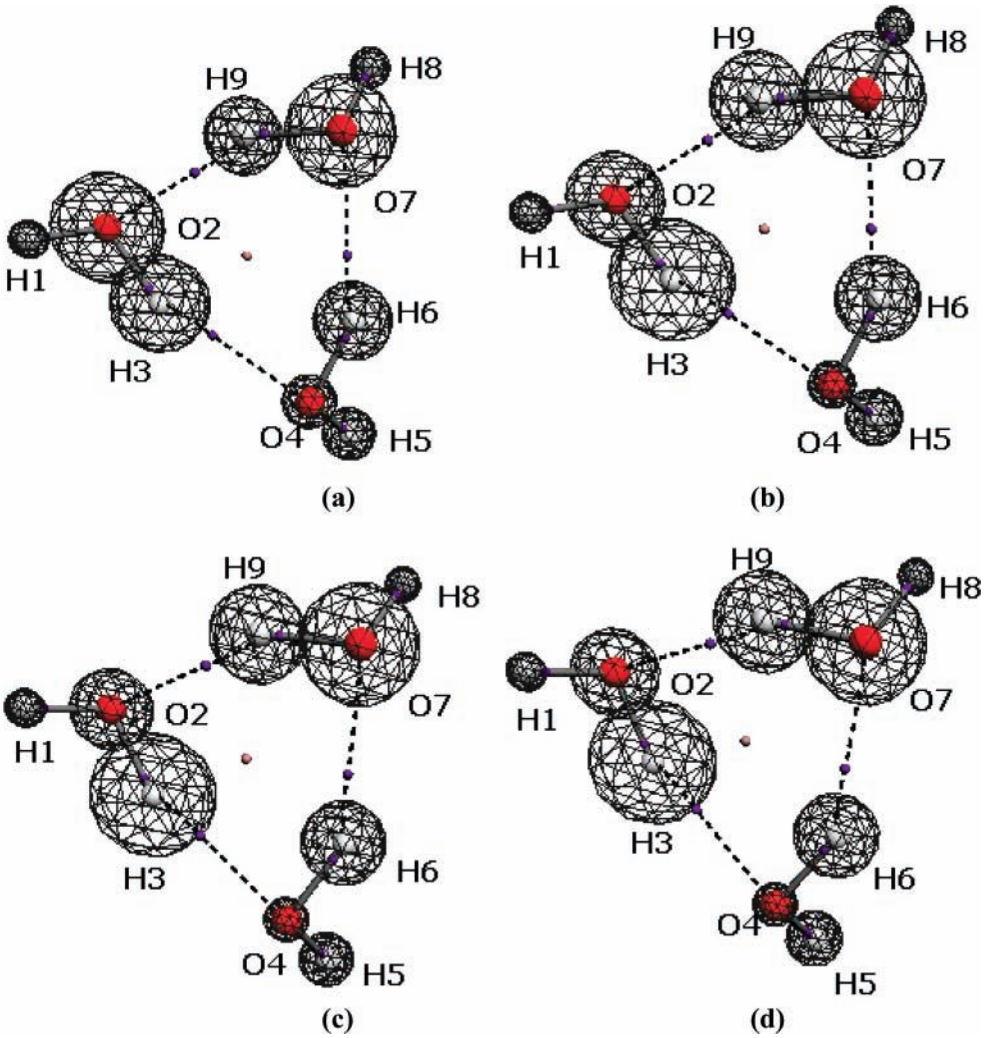

Figure 7. Transferability of atomic multipole moments in the water trimer with a cutoff of (a) $\rho = 10^{-3}$ au, (b) $\rho = 10^{-4}$ au, (c) $\rho = 10^{-5}$ au, and (d) $\rho = 10^{-7}$ au. The size of the triangulated spheres represents the average energy difference between the interactions of supermolecule and the fragments.

Since they do not extend to the most outer regions of the molecule, they cannot be dented and distorted by topologically distant atoms. As an added bonus, truncated atoms are also faster and easier to represent visually with our recently developed finite element method, and they are in line with the older and familiar pictures generated at the $\rho = 10^{-3}$ au cutoff.

Now we address the second question. We are now looking at the transferability of an atom appearing in a supermolecule and in the corresponding superposition of isolated constituent molecules. For this purpose, we generated a wave function for the supermolecule Ser...$(H_2O)_5$ on one hand and wave functions for an isolated serine and an isolated water pentamer on its own (without serine) on the other hand. The supermolecule (Ser...-$(H_2O)_5$) is thus separated into two noninteracting fragments. The positions of the nuclei in the two isolated fragments (serine and $(H_2O)_5$) are identical to those of the cluster (Ser...$(H_2O)_5$). We obtained the electrostatic multipole moments of the atoms in all three wave functions. Then, for a given atom, its interaction energy with other atoms in the system (including those in the same fragment) is calculated and averaged. This value is then compared between the two systems: the supermolecule on one hand and the two fragments that constitute this supermolecule on the other. These values are tabulated in Table 1 for two different electron density cutoff values. They are also shown in Figure 6a ($\rho = 10^{-4}$ au) and Figure 6b ($\rho = 10^{-7}$ au). By means of this table and figure, one can assess transferability from atom−atom interaction energies.

The energy differences are never less than 1 kJ/mol but can amount up to 20 kJ/mol. The values for $\rho = 10^{-4}$ au are quite similar to those for $\rho = 10^{-7}$ au, often differing by only a few tenths of a kJ/mol. Most affected by this cutoff difference is the alcohol oxygen of serine (O10), where there is a discrepancy of 3 kJ/mol. The atoms in the border between the two fragment systems, serine and $(H_2O)_5$, are poorly transferable. In particular, three atoms involved in intermolecular hydrogen bonds, O10, H11, and H16, show an average difference greater than 12 kJ/mol. Surprisingly, the fourth atom involved in these hydrogen bonds, O18, presents an average energy difference of only 3.3 kJ/mol. Overall, the atoms of serine are more transferable from the isolated serine to the supermolecule than the atoms in the water cluster. This is especially true for serine's hydrogen atoms, where the total average difference is 2.2 kJ/mol (without H11). In the water cluster, H29 has the lowest energy difference (2.1 kJ/mol), the average being 4.6 kJ/mol (if H16 is excluded). The water cluster is more polarizable than serine, which can explain the difference in transferability behavior. The overall energy, averaged over all atoms, is roughly the same between the two cutoff values, $\rho = 10^{-4}$ and $\rho = 10^{-7}$ au, namely, 5.9 and 5.4 kJ/mol, respectively. This energy difference is largely due (neglecting the BSSE) to polarization (in the sense of electron

density reorganization), which is of course present in the supermolecular wave function but not in the superimposed fragment wave functions (i.e., serine and $(H_2O)_5$).

Finally, we carry out the same analysis for the water trimer, which is split into a monomer (H1−O2−H3) with its own wave function and the remaining dimer again with its own wave function. As before, atom−atom interaction energies in this fragmented cluster are compared with those in a supermolecule in which the nuclear positions are identical. The results are shown in Table 2 and the accompanying Figure 7. For most atoms, there is very little difference in the transferability of the interaction energy, computed at the four different electron density cutoff values ($\rho = 10^{-n}$ au, $n = 3$, 4, 5, or 7). Atoms O2 and H3, which are both involved in hydrogen bonding, are most affected but oppositely. The atom O2 is less transferable at the cutoff value of $\rho = 10^{-3}$ au than at any other cutoff value while atom H3 is most transferable at $\rho = 10^{-3}$ au. Overall, the interaction energies averaged over all atoms are quite constant over all cutoff values. All atoms involved in hydrogen bonding (except O4) show an energy difference of more than 12 kJ/mol. Finally, we point out that poor transferability of a hydrogen in a hydrogen bond is compensated by good transferability of the oxygen in the same hydrogen bond. This is true both in the water trimer and the serine/water cluster.

It is clear that an accurate force field cannot ignore polarization, in spite of high-rank multipolar electrostatics and considerations of cutoff electron density. Investigations on the capability of machine learning (traditional neural networks, support vector machines, genetic programming) to capture and predict this polarization are currently underway in our lab.

The comparison of atomic multipole moments in clusters compared to those in the constituent isolated molecules is affected by the BSSE problem. In principle, this means that the electron density is likely to be different not only because of polarization but also because of the difference in the basis sets used. Salvador et al.[33] showed that no BSSE-corrected densities can be obtained via the counterpoise method however. Instead, this analysis must be carried out by using a priori methods[33,34] such as the chemical Hamiltonian approach, which is beyond the scope of this study. Fortunately, the effect of the BSSE is fairly small[33] in the presence of diffuse functions, which we used in this study.

Conclusions

For the first time, transferability of topological atoms is assessed via atom−atom (multipolar) electrostatic interaction energies by means of two systems: $(H_2O)_3$ and serine...$(H_2O)_5$. We assess this transferability in two ways: first, between different electron density cutoff values within the same system and, second, between a supermolecule and its constituent fragments, with the multipole moments taken from the wave functions of the isolated fragments. In the first transferability test, the electron density cutoff value of $\rho = 10^{-7}$ au was taken as a reference. For each order of magnitude that the electron density cutoff increases, the difference of the corresponding atom−atom interaction energies and the energies at the reference cutoff also increases by an order of magnitude. However, the total interatomic electrostatic energy indicates that this error is constant for different configurations, in which one molecule is translated. In the second transferability test, the atomic multipole moments in serine turn out to be more transferable than those of the water cluster, with the exception of the hydroxyl group. In hydrated serine, the water cluster is more polarizable than serine, The effect of polarization on atoms participating in hydrogen bonding is quantified.

Acknowledgment. We thank the Leverhulme Trust for the financial support toward one of us (M.R.).

References and Notes

(1) Popelier, P. L. A.; Devereux, M.; Rafat, M. *Acta Crystallogr.* **2004**, *A60*, 427.

(2) Bader, R. F. W. *Atom in Molecules. A Quantum Theory*; Oxford Univ. Press: 1990.

(3) Popelier, P. L. A. *Atoms in Molecules. An Introduction*; Pearson: London, 2000.

(4) Mandado, M.; Vila, A.; Grana, A. M.; Mosquera, R. A.; Cioslowski, J. *Chem. Phys. Lett.* **2003**, *371*, 739.

(5) Grana, A. M.; Mosquera, R. A. *J. Chem. Phys.* **2000**, *113*, 1492.

(6) Vila, A.; Mosquera, R. A. *J. Chem. Phys.* **2001**, *115*, 1264.

(7) Mandado, M.; Grana, A. M.; Mosquera, R. A. *J. Mol. Struct: THEOCHEM* **2002**, *584*, 221.

(8) Lopez, J. L.; Mandado, M.; Grana, A. M.; Mosquera, R. A. *Int. J. Quantum Chem.* **2002**, *86*, 190.

(9) Vila, A.; Carballo, E.; Mosquera, R. A. *Can. J. Chem.* **2000**, *12*, 1535.

(10) Matta, C. F.; Bader, R. F. W. *Proteins: Struct., Funct., Genet.* **2000**, *40*, 310.

(11) Matta, C. F.; Bader, R. F. W. *Proteins: Struct., Funct., Genet.* **2002**, *48*, 519.

(12) Matta, C. F.; Bader, R. F. W. *Proteins: Struct., Funct., Genet.* **2003**, *52*, 360.

(13) Popelier, P. L. A.; Aicken, F. M. *Chem.—Eur. J.* **2003**, *9*, 1207.

(14) Popelier, P. L. A.; Aicken, F. M. *J. Am. Chem. Soc.* **2003**, *125*, 1284.

(15) Popelier, P. L. A.; Aicken, F. M. *ChemPhysChem* **2003**, *4*, 824.

(16) Breneman, C. M.; Thompson, T. R.; Rhem, M.; Dung, M. *Comput. Chem.* **1994**, *19*, 161.

(17) Breneman, C. M.; Rhem, M. *J. Comput. Chem.* **1997**, *18*, 182.

(18) Kosov, D. S.; Popelier, P. L. A. *J. Phys. Chem. A* **2000**, *104*, 7339.

(19) Kosov, D. S.; Popelier, P. L. A. *J. Chem. Phys.* **2000**, *113*, 3969.

(20) Popelier, P. L. A.; Rafat, M. *Chem. Phys. Lett.* **2003**, *376*, 148.

(21) Rafat, M.; Popelier, P. L. A. *J. Chem. Phys.* **2005**, *123*, 204103.

(22) Popelier, P. L. A.; Joubert, L.; Kosov, D. S. *J. Phys. Chem. A* **2001**, *105*, 8254.

(23) Joubert, L.; Popelier, P. L. A. *Phys. Chem. Chem. Phys.* **2002**, *4*, 4353.

(24) Popelier, P. L. A.; Kosov, D. S. *J. Chem. Phys.* **2001**, *114*, 6539.

(25) Rafat, M.; Popelier, P. L. A. In *Quantum Theory of Atoms in Molecules*; Matta, C. F., Boyd, R. J., Eds.; Wiley-VCH: Weinheim, Germany, 2007.

(26) Rafat, M.; Popelier, P. L. A. *J. Chem. Phys.* **2006**, *124*, 144102.

(27) Rafat, M.; Popelier, P. L. A. *J. Comput. Chem.*, in press.

(28) Rafat, M.; Popelier, P. L. A. *J. Comput. Chem.*, in press.

(29) Stone, A. J. *The Theory of Intermolecular Forces*; Clarendon: Oxford, U.K., 1996.

(30) Frisch, M. J.; Trucks, G. W.; Schlegel, H. B.; Scuseria, G. E.; Robb, M. A.; Cheeseman, J. R.; Montgomery, J. A. J.; Vreven, J. T.; Kudin, K. N.; Burant, J. C.; Millam, J. M.; Iyengar, S. S.; Tomasi, J.; Barone, V.; Mennucci, B.; Cossi, M.; Scalmani, G.; Rega, N.; Petersson, G. A.; Nakatsuji, H.; Hada, M.; Ehara, M.; Toyota, K.; Fukuda, R.; Hasegawa, J.; Ishida, M.; Nakajima, T.; Honda, Y.; Kitao, O.; Nakai, H.; Klene, M.; Li, X.; Knox, J. E.; Hratchian, H. P.; Cross, J. B.; Adamo, C.; Jaramillo, J.; Gomperts, R.; Stratmann, R. E.; Yazyev, O.; Austin, A. J.; Cammi, R.; Pomelli, C.; Ochterski, J. W.; Ayala, P. Y.; Morokuma, K.; Voth, G. A.; Salvador, P.; Dannenberg, J. J.; Zakrzewski, V. G.; Dapprich, S.; Daniels, A. D.; Strain, M. C.; Farkas, O.; Malick, D. K.; Rabuck, A. D.; Raghavachari, K.; Foresman, J. B.; Ortiz, J. V.; Cui, Q.; Baboul, A. G.; Clifford, S.; Cioslowski, J.; Stefanov, B. B.; Liu, G.; Liashenko, A.; Piskorz, P.; Komaromi, I.; Martin, R. L.; Fox, D. J.; Keith, T.; Al-Laham, M. A.; Peng, C. Y.; Nanayakkara, A.; Challacombe, M.; Gill, P. M. W.; Johnson, B.; Chen, W.; Wong, M. W.; Gonzalez, C.; Pople, J. A. *GAUSSIAN03*; Gaussian, Inc.: Pittsburgh, PA, 2003.

(31) MORPHY01, a program written by P.L.A. Popelier with a contribution from R. G. A. Bone, D. S. Kosov, and M.in het Panhuis, UMIST, Manchester, U.K., EU, 2000.

(32) Rafat, M. Towards a Force Field based on Quantum Chemical Topology. Ph.D. thesis, Manchester, U.K., 2005.

(33) Salvador, P.; Fradera, X.; Duran, M. *J. Chem. Phys.* **2000**, *112*, 10106.

(34) Salvador, P.; Duran, M.; Fradera, X. *J. Chem. Phys.* **2002**, *116*, 6443.